

Large Changes in Sea Ice Triggered by Small Changes in Atlantic Water Temperature

MARI F. JENSEN

Department of Earth Science, University of Bergen and Bjerknes Centre for Climate Research, Bergen, Norway

KERIM H. NISANCIOGLU

Department of Earth Science, University of Bergen and Bjerknes Centre for Climate Research, Bergen, and Department of Geosciences, University of Oslo, and Center for Earth Evolution and Dynamics, Oslo, Norway

MICHAEL A. SPALL

Woods Hole Oceanographic Institution, Woods Hole, Massachusetts

(Manuscript received 24 November 2017, in final form 1 March 2018)

ABSTRACT

The sensitivity of sea ice to the temperature of inflowing Atlantic water across the Greenland–Scotland Ridge is investigated using an eddy-resolving configuration of the Massachusetts Institute of Technology General Circulation Model with idealized topography. During the last glacial period, when climate on Greenland is known to have been extremely unstable, sea ice is thought to have covered the Nordic seas. The dramatic excursions in climate during this period, seen as large abrupt warming events on Greenland and known as Dansgaard–Oeschger (DO) events, are proposed to have been caused by a rapid retreat of Nordic seas sea ice. Here, we show that a full sea ice cover and Arctic-like stratification can exist in the Nordic seas given a sufficiently cold Atlantic inflow and corresponding low transport of heat across the Greenland–Scotland Ridge. Once sea ice is established, continued sea ice formation and melt efficiently freshens the surface ocean and makes the deeper layers more saline. This creates a strong salinity stratification in the Nordic seas, similar to today's Arctic Ocean, with a cold fresh surface layer protecting the overlying sea ice from the warm Atlantic water below. There is a nonlinear response in Nordic seas sea ice to Atlantic water temperature with simulated large abrupt changes in sea ice given small changes in inflowing temperature. This suggests that the DO events were more likely to have occurred during periods of reduced warm Atlantic water inflow to the Nordic seas.

1. Introduction

The forcing mechanisms behind the abrupt climate changes occurring repeatedly during the last ice age, the Dansgaard–Oeschger (DO) events, are still debated. The DO events were first identified in ice cores on Greenland, where the events are characterized by an abrupt warming of $10^{\circ} \pm 5^{\circ}\text{C}$ in a few decades (Johnsen et al. 1992; Dansgaard et al. 1993; North Greenland Ice Core Project members 2004). During the glacial period, the climate of Greenland alternated between cold stadial and warm interstadial conditions with a period of roughly 1500 years (Groote and Stuiver 1997). Further

climate reconstructions suggested a global extent [see Voelker (2002) and Rahmstorf (2002) for an overview] with, for example, warmer and wetter climate in Europe coinciding with interstadial conditions on Greenland.

Climate reconstructions show large variations in the North Atlantic during the same time period with, for example, sea surface temperature changes of 10°C (Sánchez Goñi et al. 2008) and movements of ocean fronts (Eynaud et al. 2009; Voelker and de Abreu 2013; Rasmussen et al. 2016) occurring with the Greenland stadial–interstadial cycles. Originally, a change in the Atlantic meridional overturning circulation (AMOC) was proposed as a mechanism explaining the millennial-scale climate variability (Broecker et al. 1990; Tziperman 1997; Marotzke 2000; Ganopolski and Rahmstorf 2001). However, it is not clear how a change in AMOC alone can initiate a 10°C warming on Greenland. In recent years, the agent for the warming on Greenland is believed

 Denotes content that is immediately available upon publication as open access.

Corresponding author: Mari F. Jensen, mari.f.jensen@uib.no

DOI: 10.1175/JCLI-D-17-0802.1

© 2018 American Meteorological Society. For information regarding reuse of this content and general copyright information, consult the [AMS Copyright Policy](https://www.ametsoc.org/PUBSReuseLicenses) (www.ametsoc.org/PUBSReuseLicenses).

to be abrupt reductions in sea ice cover (Broecker 2000; Gildor and Tziperman 2003; Masson-Delmotte et al. 2005), in particular over the Nordic seas (Li et al. 2005; Dokken et al. 2013). During stadial conditions on Greenland, the Nordic seas are hypothesized to be fully sea ice covered, thereby insulating the relatively warm ocean from the cold atmosphere above. An abrupt reduction in sea ice cover leads to a rapid release of oceanic heat to the atmosphere. In particular, model studies show a 7°C warming on Greenland resulting from sea ice loss in the Nordic seas (Li et al. 2005, 2010). Li et al. (2005) also show that the reconstructed changes in snow accumulation on Greenland during DO events can be explained by abrupt reductions in sea ice cover.

An increasing number of climate reconstructions from marine sediment cores support the existence of a temporal sea ice cover in the Nordic seas during the last glacial period (Dokken et al. 2013; Hoff et al. 2016). In particular, Dokken and Jansen (1999), Rasmussen and Thomsen (2004), Dokken et al. (2013), and Ezat et al. (2014) show that the hydrography of the eastern Nordic seas during stadial conditions resembles the Arctic Ocean today, with a warm subsurface below a cold and fresh surface layer, which is a stratification that may allow for the presence of a sea ice cover (Jensen et al. 2016). During warm interstadials, the Nordic seas are shown to be less stratified, with warm Atlantic water close to the surface. Recently, direct evidence for the presence of sea ice at the same sites is emerging; for example, sea ice biomarkers have been found in oceanic sediments (Hoff et al. 2016).

Today, the eastern Nordic seas are free of sea ice, and the surface ocean is significantly warmer than other oceans at similar latitudes (Hansen and Østerhus 2000). Warm Atlantic water enters the Nordic seas over the Greenland–Scotland Ridge (GSR) and the Norwegian Atlantic Current carries heat and salt toward the Arctic Ocean along the coast of Norway (Orvik and Niiler 2002; see Fig. 1 herein). The result is an eastern Nordic seas with a temperature of approximately 8°C, even in winter (Hansen and Østerhus 2000; Seidov et al. 2013, 2015). Heat is continuously lost to the atmosphere as the current travels northward. However, climate reconstructions of the last glacial period show a temporal, seasonal sea ice cover off the coast of Norway (Hoff et al. 2016). There must have been changes to the hydrography and vertical stratification of the Nordic seas to allow for the existence of sea ice here. Either the incoming Atlantic water cooled substantially, the volume of warm Atlantic inflow was reduced, or the Atlantic water entered the Nordic seas at greater depths.

Here we study the existence and stability of sea ice in the Nordic seas by applying an idealized eddy-resolving configuration of the Massachusetts Institute of

Technology General Circulation Model (MITgcm). A similar setup without sea ice has been shown to reproduce most of the characteristic of the modern circulation in the Nordic seas (Walín et al. 2004; Spall 2004, 2011, 2012); in particular, both the observed barotropic and baroclinic part of the boundary current (Orvik et al. 2001) were reproduced by Walín et al. (2004). The warm cyclonic boundary current in the Nordic seas exists because of topography and surface buoyancy forcing. Wind is shown to have little impact on the exchange between the subpolar Atlantic and the Nordic seas (Spall 2011). Eddies, on the other hand, carry heat both across the GSR and into the interior of the Nordic seas and are critical for a realistic representation of the heat exchanges in the area. A coupled ocean–sea ice setup of this model has been applied to study an Arctic Ocean–like domain (Spall 2013). This version is used here to study the Nordic seas and the potential for abrupt changes in sea ice during cold glacial climates.

Our study suggests that a full sea ice cover can exist in the Nordic seas given a reduction in the poleward heat transport across the Greenland–Scotland Ridge. Details of the model are given in section 2, while the results of the experiments and the stability of a Nordic seas sea ice cover are assessed in section 3. The implications of the results for our understanding of the DO events are discussed in section 4.

2. An idealized numerical model of the Nordic seas

We apply an idealized eddy-resolving version of the MITgcm to study the existence of sea ice in the Nordic seas. The model configuration with an idealized Nordic seas basin is shown in Fig. 2. There is no interactive atmosphere; instead, sea surface temperatures are restored toward constant atmospheric temperatures, with a maximum of 10°C in the south and a minimum of −20°C in the north (Fig. 2). Note that there are no time variations in atmospheric forcing; we are in essence studying a constant winter. To keep it simple, precipitation and wind are not included. The reader is referred to Spall (2011, 2012), who found that wind forcing has a minor impact on the heat exchange between the basins compared to buoyancy forcing. The bathymetry consists of sloping sides, with a maximum depth of 2000 m and a 1000-m-deep ridge. The domain is divided into two subdomains, one south and one north of the ridge. The basin north of the ridge is hereafter referred to as the Nordic seas, the focus area of this study.

The horizontal resolution is 5 km, and there are 30 vertical layers; the upper 20 layers are 50 m, and the deepest 10 layers are 100 m thick. We apply a realistic

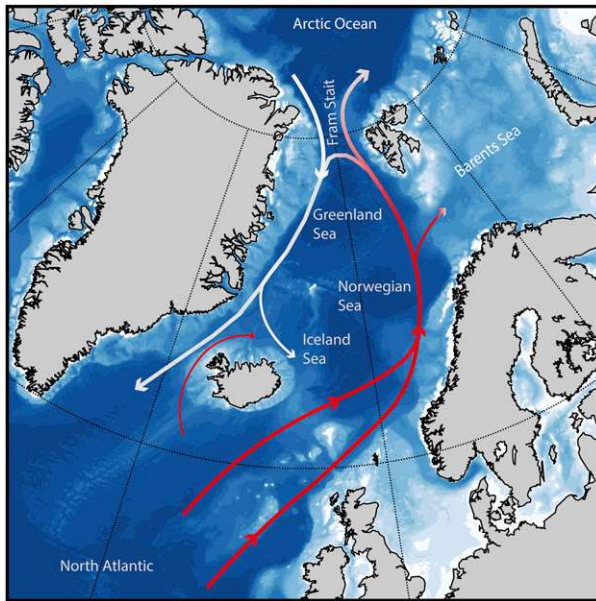


FIG. 1. The modern configuration of the Nordic seas and northern North Atlantic. Lines with arrows indicate the general surface circulation of the area, based on Hansen and Østerhus (2000). The colors of the lines indicate the temperature of the current where red is warmer than white. Figure adapted from Jensen (2017).

equation of state; the density is calculated with the Jackett and McDougall (1995) formula, a constant Coriolis parameter, $f = 1.2 \times 10^{-4} \text{ s}^{-1}$, and vertical diffusivity and viscosity of $1 \times 10^{-5} \text{ m}^2 \text{ s}^{-1}$. Convection is parameterized with implicit vertical diffusion; the diffusivity increases to $1000 \text{ m}^2 \text{ s}^{-1}$ for statically unstable conditions. Horizontal viscosity is parameterized using the Smagorinsky closure (Smagorinsky 1963):

$$A_h = (v_s/\pi)^2 \Delta^2 [(u_x - v_y)^2 + (v_x + u_y)^2]^{1/2},$$

where $v_s = 2.5$ is a nondimensional coefficient, Δ is the horizontal grid spacing, and u and v are the zonal and meridional velocities, respectively, with subscripts x and y indicating partial differentiation. Typical values are $30 \text{ m}^2 \text{ s}^{-1}$ for the boundary current region. Temperature and salinity are advected using a third-order flux-limiting scheme.

A new feature of this study is that the domain is coupled to a zero-layer thermodynamic sea ice model with viscous-plastic dynamics (Hibler 1980; Zhang and Hibler 1997; Losch et al. 2010). The sea ice model has been included in an Arctic Ocean–like setup where many physical aspects of the Arctic circulation are represented (Spall 2013) but has not been applied to the Nordic seas domain. To mimic river runoff, Spall (2013) included a virtual freshwater forcing that is not included in this study. We are thus studying a sea ice cover in the

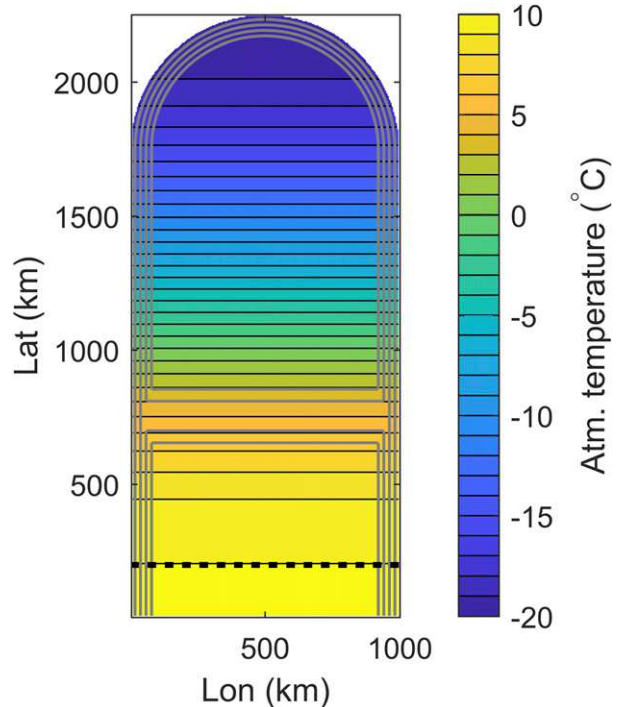


FIG. 2. The model setup. Colors show the atmospheric temperature toward which the sea surface temperatures are restored. South of the black dashed line salinity is restored to 35 psu and oceanic temperature is restored to values in the range 1° – 8°C , representing changes in inflowing Atlantic water temperature. Gray contours (every 300 m) outline the ocean bathymetry. The northern basin is considered to represent the Nordic seas, separated from the North Atlantic by a sill at a depth of 1000 m.

absence of external freshwater supplies. The sea ice is assumed not to store any heat, there is no snow, and the salinity of the ice is set to 0 psu. Atmospheric restoring is deactivated over sea ice; instead a constant downward longwave radiation $F_{LW\downarrow}$ of 60 W m^{-2} is specified where there is sea ice present. The temperature of the sea ice surface T_s is solved to balance $F_{LW\downarrow} + F_c(T_s) - F_{LW\uparrow}(T_s) = 0$, where F_c is the heat conduction through the sea ice, and $F_{LW\uparrow}$ is the upward longwave radiation.

We assume an infinite amount of warm Atlantic water present in the south by restoring the southern boundary to constant temperatures (between 1° and 8°C) and salinities (35 psu) with a restoring strength of $40 \text{ W m}^{-2} \text{ C}^{-1}$ and a time scale of 1 month. The model is initialized from rest with a constant salinity of 35 psu, and a temperature corresponding to the restoring temperature at all depths.

We perform eight main simulations where the restoring temperature in the south (hereafter referred to as the Atlantic water temperature or T_A) varies between 1° and 8°C . The runs are named XXDEG, where XX is the restoring temperature in degrees Celsius (Table 1). The 4.5DEG–8DEG simulations are run for 60 years, the

TABLE 1. List of experiments. Heat transport is net across sill crest. The row with numbers in italics is 5-yr averages of minimum sea ice cover conditions.

Name	T_A (°C)	Heat transport (TW)			Sea ice volume (km ³)	Max NMOC (Sv)
		Total	Mean	Eddy		
1DEG	1	53	22	31	4158	2.4
2DEG	2	63	23	40	3634	2.4
3DEG (COLD)	3	70	20	50	3193	2.3
4DEG	4	82	24	58	2578	2.6
	—	<i>187</i>	<i>33</i>	<i>154</i>	<i>1088</i>	<i>4.5</i>
4.5DEG	4.5	226	36	190	944	5.3
5DEG	5	260	46	214	809	6.0
6DEG (WARM)	6	364	80	284	475	8.1
8DEG	8	519	104	415	168	9.6

1DEG–3DEG simulations are run for 120 years, and the 4DEG experiment that exhibits transient changes in sea ice volume is run for 200 years. All figures (if not specified otherwise) are time averages over 10 years.

3. Results

First, we investigate the circulation of the Nordic seas domain and the features common to all experiments by using the 6DEG experiment (section 3a) as a reference. Thereafter, we describe the formation of an extensive sea ice cover (section 3b) and its implications for the ocean circulation (section 3c). Theoretical considerations are presented in section 3d.

a. Nordic seas circulation

The buoyancy forcing from atmospheric cooling in the north and warming in the south drives a warm baroclinic inflow to the Nordic seas from the warmer southern domain. The warm water crosses the sill on the western side over the open geostrophic contours, before it travels eastward on the northern sill flank (Fig. 3). Thereafter, the warm water flows cyclonically along the topographic contours around the Nordic seas, similar to the circulation today (Figs. 3 and 4). South of the ridge, the circulation consists of both a cyclonic and an anticyclonic gyre (Fig. 3).

We note that in today's Nordic seas, the northward flow of warm water across the GSR mainly takes place on the eastern side of the ridge. However, we are interested in the total heat transport into the Nordic seas and the circulation of the Nordic seas itself. As there are no zonal variations in atmospheric temperature, the total heat transport across the GSR is not affected by the location of the inflow. In addition, as the circulation within the Nordic seas–like domain resembles observations, we argue that the inflow on the western side is not critical for our main results. Walin et al. (2004) show a similar circulation in an idealized two-basin setup without

wind, while still being able to model the main characteristics of the Nordic seas. We therefore focus on the circulation within the Nordic seas itself and the amount of heat entering the basin.

Exchange of heat across the GSR is secured by the mean flow and eddy heat fluxes, with the latter dominating

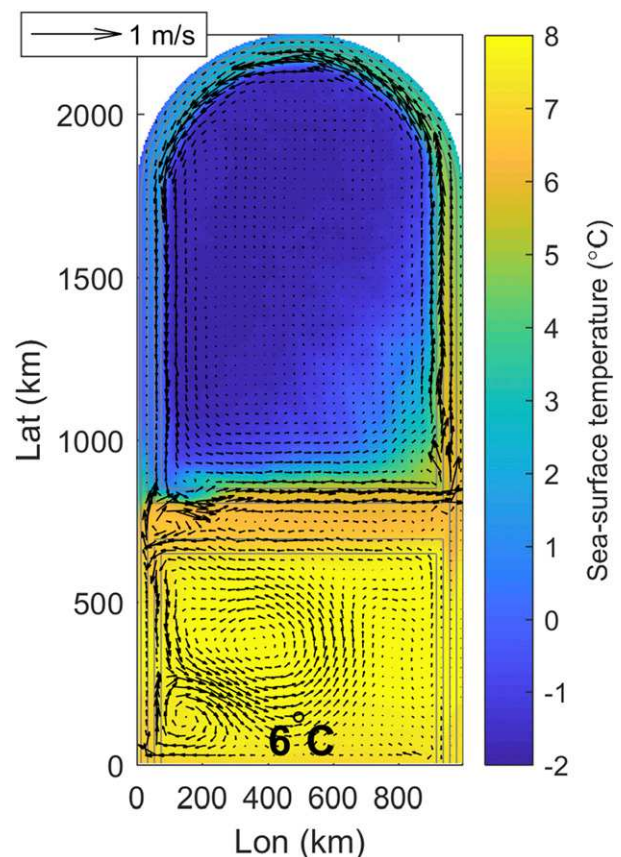


FIG. 3. Colors show sea surface temperatures in experiment 6DEG. Black arrows represent the mean speed over the upper 450 m, plotted every 30 km. Gray lines show bathymetry. The circulation is dominated by a warm cyclonic boundary current.

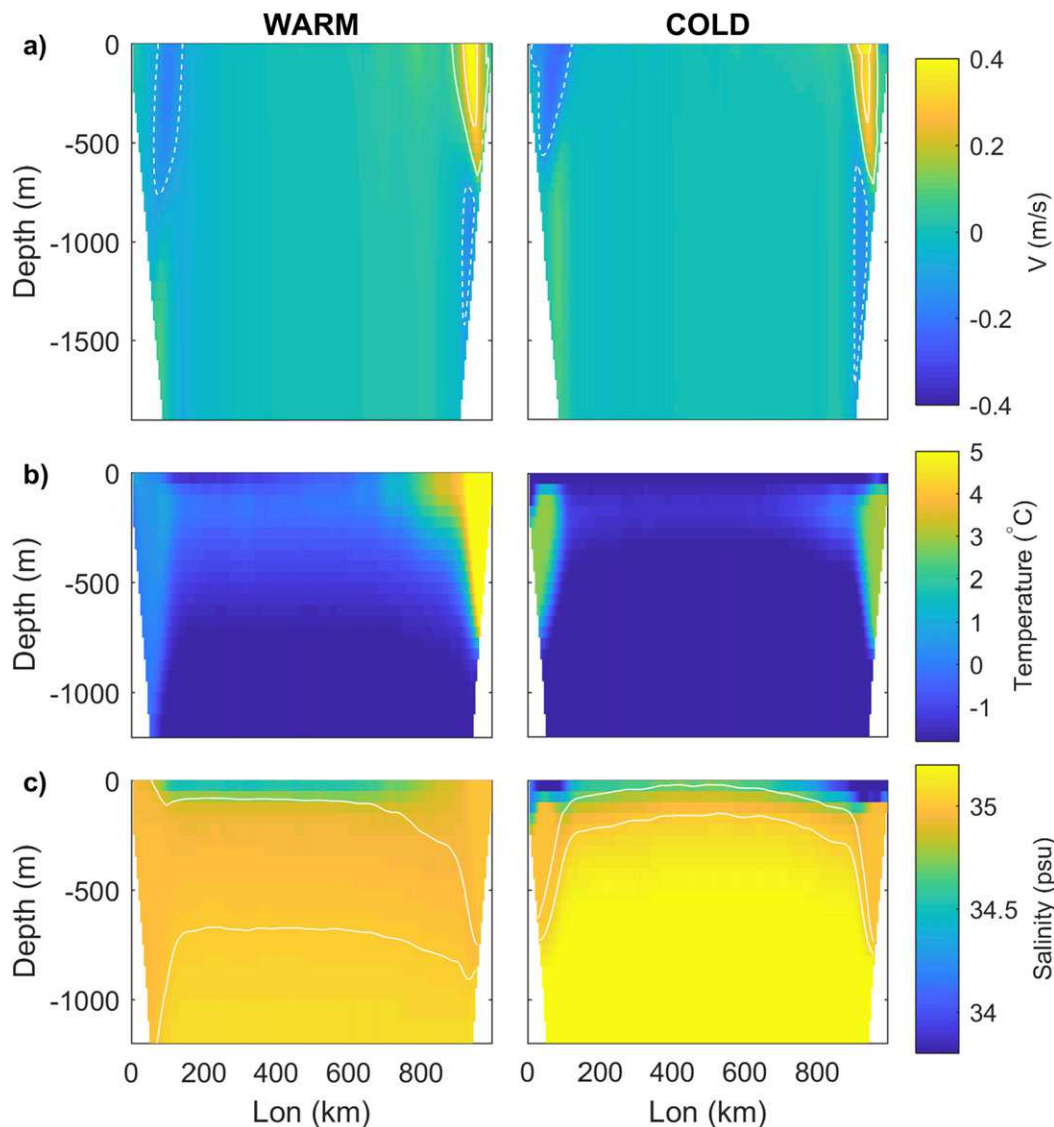


FIG. 4. Colors show (a) meridional velocity, (b) temperature, and (c) salinity in the Nordic seas (at 1000 km north, latitudinal direction) for (left) 6DEG and (right) 3DEG. Solid and dashed lines in (a) mark velocities of $+0.1$ and $+0.3 \text{ m s}^{-1}$ and -0.1 m s^{-1} , respectively. The density contours 1028 and 1028.2 kg m^{-3} are marked in white in (c). Both 3DEG and 6DEG have a cyclonic boundary circulation above the sill depth that is set to 1000 m .

the total heat transport into the Nordic seas (Fig. 5). The total heat transport is calculated as

$$\int_0^X \int_{-H}^0 \rho c_p v T dz dx, \quad (1)$$

where ρ is the density, c_p is the heat capacity of seawater, and T is the temperature (referenced to 0°C). The integration is carried out over the full depth H and across the entire sill crest ($X = 1000 \text{ km}$). As v and T can be divided into their mean and residual components, the total heat transport can be divided into that caused by the mean flow

and that from eddy heat fluxes (Fig. 5). Eddy heat fluxes contribute two-thirds of the total heat transport across the ridge, and originate from the unstable temperature front across the sill crest. However, in the inflow region (the westernmost 100 km) the mean flow dominates the heat transport [Fig. 5; Eq. (1) with $X = 100 \text{ km}$]. Here, warm water is advected northward with the mean flow, except for a cold outflow at depth. Along the rest of the sill crest, eddy heat fluxes carry heat northward and are thus crucial for a correct representation of the net heat exchange.

North of the sill, the main northward flow is confined to a baroclinic eastern boundary current (here defined as

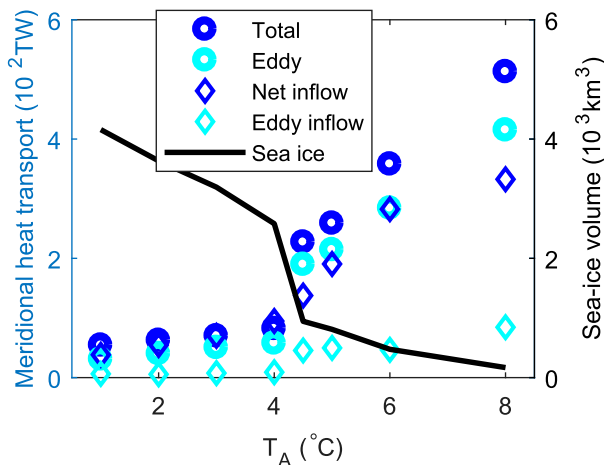


FIG. 5. Total heat transport and heat transport in the inflow (westernmost 100 km, relative to 0°C) across the sill crest for all experiments. Both the net heat transport (mean + eddy) and the contribution from eddies are shown. The total sea ice volume for each experiment is shown with the black line.

the easternmost 100 km and 250–1000 km north of the sill), while the southward flow is both in the upper part of the western boundary current (defined as the westernmost 100 km and 250–1000 km north of the sill), and at depths in the eastern boundary current (Fig. 4). The horizontal extent is limited by the sloping bathymetry.

Below sill depth (1000 m) there is a weak anticyclonic boundary current. Walin et al. (2004) also find an anticyclonic vortex in the deep with very little relevance for the surface circulation. There is also a weak barotropic cyclonic gyre off the sloping bathymetry (as seen in oceanographic observations; Orvik et al. 2001).

The interior of the Nordic seas domain is not connected to the southern domain via open geostrophic contours. As a consequence, the net heat transport in the interior is mainly driven by eddy heat fluxes. The unstable baroclinic boundary current sheds off eddies to the interior. However, the cold atmosphere manages to cool down the interior to the freezing point, making the interior the coldest part of the Nordic seas. For all experiments, sea ice is present in the interior of the Nordic seas (Fig. 6) because of the cold atmosphere and limited heat transport into the interior.

b. Sea ice–induced halocline formation

Although the main circulation remains the same for all experiments, the different Atlantic water temperatures lead to two distinctly different states for the Nordic seas: one where the entire domain is covered in sea ice (1DEG–4DEG; Fig. 6) and one where only the interior is sea ice covered while the margins are ice free (4.5DEG–8DEG; Fig. 6). The states are hereafter referred to as COLD and WARM, and represented by the 3DEG and 6DEG

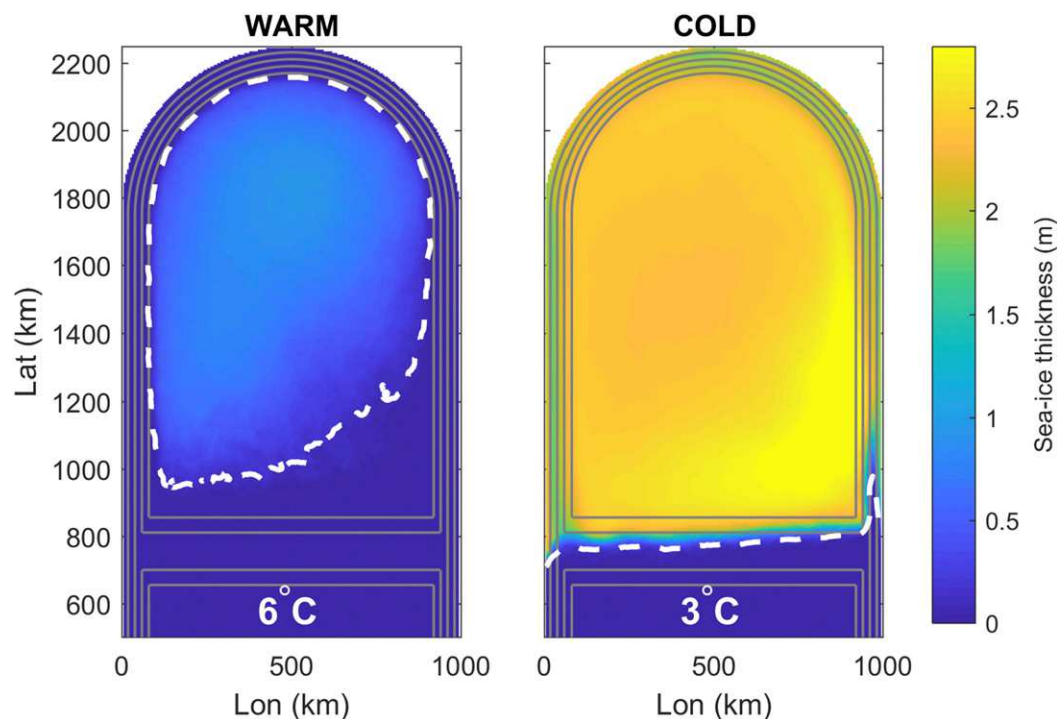


FIG. 6. Colors show sea ice thickness for (left) 6DEG and (right) 3DEG. The dashed white line marks the zero-contour line for sea ice thickness, and gray lines show bathymetry. For the COLD experiments the entire northern domain is covered in sea ice, while only the interior has a sea ice cover for the WARM experiments.

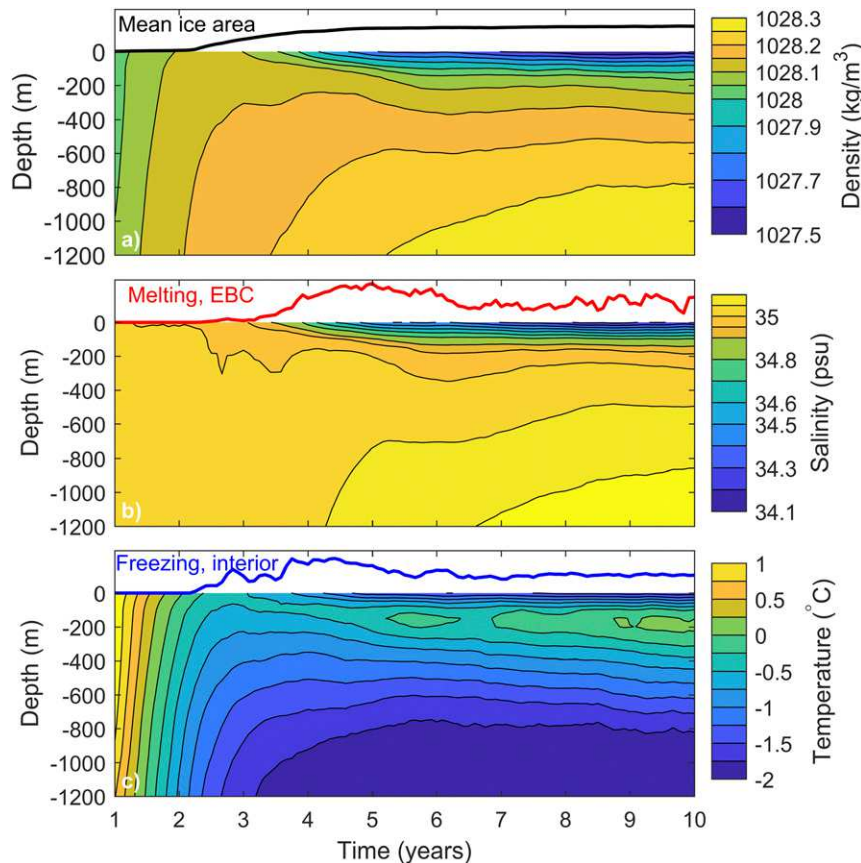


FIG. 7. Hovmöller diagram with (a) density, (b) salinity, and (c) temperature for years 1–10 for 3DEG (COLD) averaged over the Nordic seas. Lines in the top part of each panel show mean sea ice area, total sea ice melting in the eastern boundary current (EBC), and sea ice production in the interior of the Nordic seas in (a)–(c), respectively. The sea ice melting produces a fresh surface layer that dominates the stratification.

experiments, respectively. Within each subset, the differences between experiments are much smaller and more gradual than differences between the two different states.

For the WARM experiments, both the net heat transport and the total sea ice volume change close to linearly with Atlantic water temperatures (Fig. 5). The change in sea ice volume is mainly a result of sea ice thickness changes, but also a result of greater sea ice area: As the warm cyclonic boundary current cools by heat loss to the atmosphere and by eddy fluxes to the interior, the sea ice extends farther out into the warm boundary current. When moving to lower Atlantic water temperatures, the linear decrease in heat transport is mainly the result of a decrease in eddy heat fluxes as the north–south temperature gradient decreases, and a linear decrease in the velocity of the boundary current.

In contrast, changes in the heat transport and sea ice volume are highly nonlinear when transitioning from the WARM to the COLD experiments (Fig. 5), suggesting that feedbacks in response to the decrease in T_A are causing the rapid expansion of sea ice. The COLD

experiments all have sea ice covering the entire Nordic seas, including the warm boundary current; the volume differences within the COLD experiments are due to sea ice thickness. We use the COLD experiment (3DEG), which has an extensive sea ice cover in the Nordic seas, to investigate how the sea ice is formed. Ice volume reaches a steady state after about 30 years. However, as sea ice area reaches its maximum after only 10 years, we will study the underlying dynamical processes during the first decade.

As the atmosphere cools the Nordic seas domain, the surface ocean becomes denser (Figs. 7a,c). Seeing that there are no freshwater sources and no precipitation added to the domain, the initial salinity is 35 psu everywhere with a freezing point of -1.9°C . This temperature is reached in the north of the domain after a few months. Sea ice formation starts, and brine rejection increases the salinity of the ocean below, leading to vigorous deep convection. As the sea ice thickens, salinity at depth increases. Given that a restoring to 35 psu is applied in the south, part of the excess salt is removed, and the restoring acts as a virtual freshwater supply.

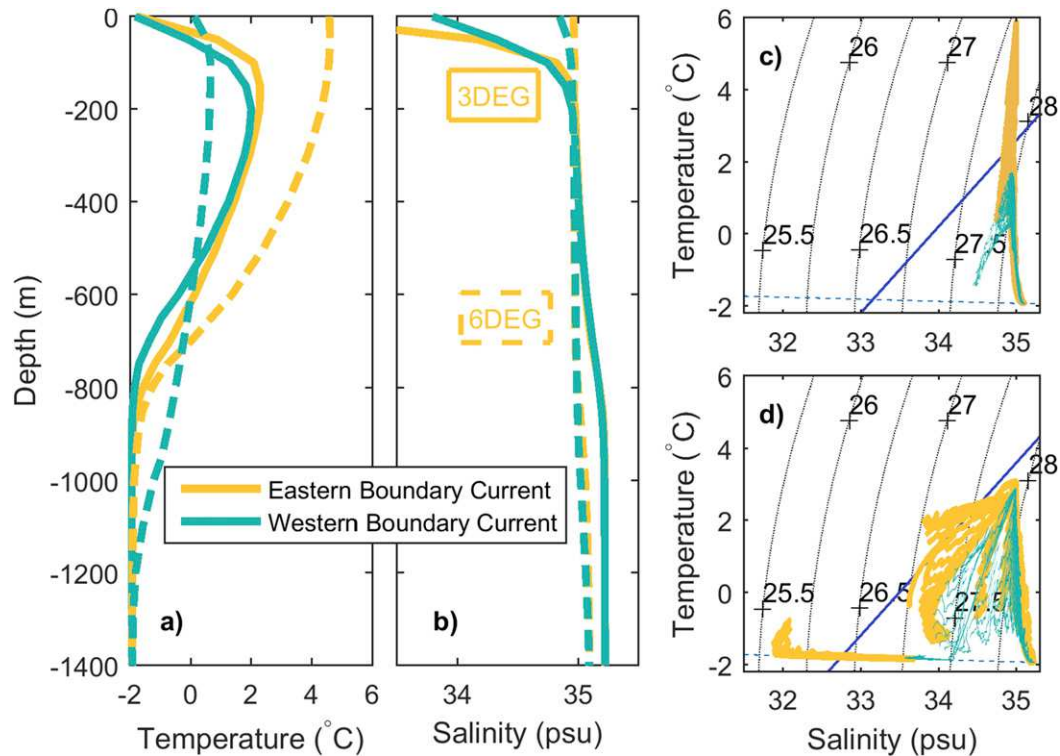


FIG. 8. (a) Temperature and (b) salinity profiles averaged over the eastern (yellow) and western (green) boundary of the basin. Solid and dashed lines represent the 3DEG and 6DEG experiments, respectively, both averaged over years 40–50. Also shown are TS diagrams for the same areas for (c) 6DEG and (d) 3DEG. In (c),(d), dotted lines mark density (kg m^{-3}), the dashed line marks the freezing point, and the solid line marks the Gade line (Gade 1979). The COLD (3DEG) experiment has a stronger halocline than the WARM (6DEG) experiment and a temperature maximum at depth.

Freshwater is stored in the newly created sea ice. When sea ice meets warm Atlantic water, it melts and releases freshwater back to the surface. As a consequence, enhanced sea ice production acts to stratify the Nordic seas by efficiently freshening the surface, and making the deeper ocean more salty and dense (Fig. 7b). The melting of sea ice lags the freezing in the beginning, but eventually the two balance each other. Sea ice is transported from the regions with active sea ice formation to the regions with sea ice melt. Thus, advection of sea ice by the ocean plays an important role for the stratification, as sea ice is advected into the warm boundary current where it melts and releases freshwater. An additional sensitivity experiment with a purely thermodynamic sea ice model (replacing the dynamic sea ice model including advection by ocean currents) resulted in sea ice existing only in the interior of the Nordic seas for all experiments (also for the COLD experiments). For the dynamic sea ice model, the mean flow dominates the total advection of sea ice, except for periods with little sea ice when eddy fluxes dominate (not shown).

As a consequence of the stratifying effect of sea ice, a halocline emerges for the COLD experiments (Figs. 7 and 8). Sufficient ice is melted to create a protective

fresh surface layer, forcing the relatively warm and salty Atlantic water to subduct as it flows north into the basin. The relatively salty and warm Atlantic waters ($>0^{\circ}\text{C}$), which dominated the surface circulation of the Nordic seas, are now more dense than the fresh surface layer and subduct to approximately 200-m depths (Figs. 7c and 8). Thus, the warm boundary current is still present in the COLD experiments, but it is located below the fresh surface layer (Fig. 4b). The ensuing stratification allows for an expansion of the sea ice cover as the fresh cold layer efficiently separates the sea ice from the warmer Atlantic water below.

The halocline is absent in the boundary current region for the WARM experiments (Fig. 8). The stratification by production and melting of sea ice also occurs in the WARM experiments where the atmosphere cools the surface ocean in the interior of the Nordic seas basin to freezing temperatures. However, the buoyancy flux from freshwater input from melting sea ice is smaller than in the COLD experiments (Fig. 9a), especially in the beginning of the experiment (not shown). In the WARM experiments, there is not enough meltwater present to create a fresh surface layer, and the warm

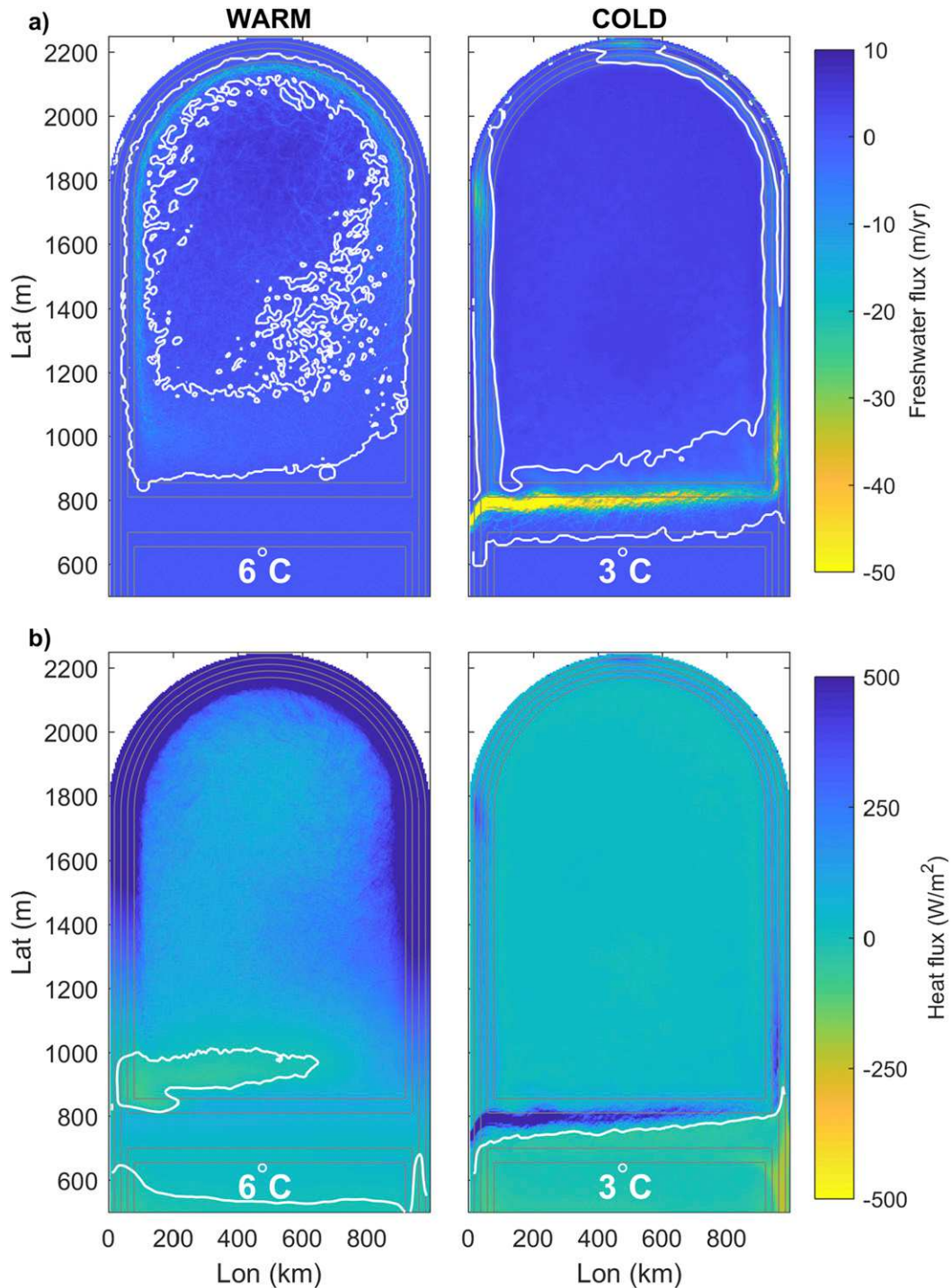


FIG. 9. Buoyancy flux resulting from (a) surface salt flux and (b) surface heat flux in (left) 6DEG and (right) 3DEG. Negative values (yellow colors) indicate more buoyant water. White lines mark the smoothed zero contour, and gray lines show bathymetry. The COLD experiments become more buoyant in the Nordic seas because of a more negative salt flux and a smaller heat flux.

Atlantic water is still at the surface in the boundary current region, preventing sea ice formation (Fig. 4). In addition, as the Atlantic water is colder for the

COLD experiments, less freshwater is needed to produce a surface layer lighter than the Atlantic water (section 3d).

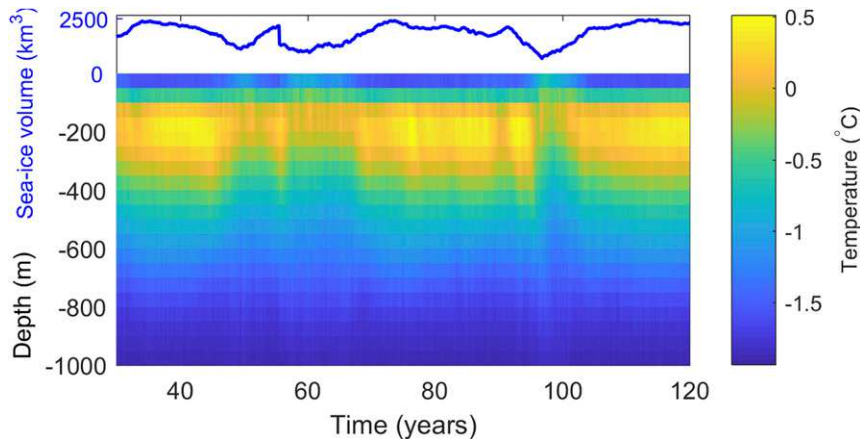


FIG. 10. Hovmöller diagram of temperature averaged over the Nordic seas for 4DEG. The blue line shows transient changes in total sea ice volume.

In summary, sea ice in the Nordic seas basin forms because of cooling by the atmosphere, and the extent is aided by advection and melting of sea ice, which creates a fresh surface layer. A halocline emerges spontaneously once the temperature of the inflowing Atlantic water is sufficiently reduced.

Interestingly, the 4DEG experiment, which is the warmest of the COLD experiments, exhibits unforced transient changes in sea ice cover (Fig. 10). The experiment shifts repeatedly between the COLD and the WARM state. For this experiment, there is just enough meltwater present to create a fresh surface layer. However, with time the subsurface becomes warmer and eventually lighter than the surface layer. As a result, warm water is mixed up and sea ice melts. The eastern and northern boundary current becomes temporarily ice free.

c. Changes in heat transport and meridional overturning circulation

The presence of an extensive sea ice cover has implications for the ocean circulation. When the boundary current area is covered by sea ice, the release of heat to the atmosphere is reduced (Fig. 9b). Hence, the western boundary current is much warmer when sea ice is present, and the warm boundary current is isolated from the atmosphere by a strong halocline (Figs. 4b and 8a). In 6DEG, the warm water has cooled by approximately 3°C when reaching the western boundary current. In 3DEG, the cooling of the warm boundary current from the eastern margin to the western margin is reduced to approximately 0.3°C. (Fig. 8a). The cooling in 6DEG is mainly attributed to eddy heat fluxes and atmospheric cooling (Fig. 8c). As parts of the temperature–salinity (TS) diagram for 3DEG follows the Gade line (density change resulting from the salinity and temperature

decrease associated with sea ice melt; Gade 1979), energy lost to sea ice melt contributes to the cooling in 3DEG (Fig. 8d). Note that below 800-m depth the western boundary is colder in 3DEG than in 6DEG.

Total heat transport into the Nordic seas is low when a full sea ice cover is present (Fig. 5). This is a result of low Atlantic water temperatures but also a consequence of the insulating sea ice cover, which reduces the temperature difference between the inflowing and outflowing water across the sill. As the release of heat to the atmosphere is reduced with a full sea ice cover, heat is recirculated within and out of the Nordic seas. In addition, the reduction in the velocities across the sill crest and in the boundary current (Fig. 4) impacts the total heat transport.

The strength of the Nordic seas meridional overturning circulation (NMOC) decreases when a full sea ice cover is present (Fig. 11). As with the net heat transport, the decrease could either be due to smaller buoyancy forcing caused by a decrease in T_A and a consequent smaller north–south temperature gradient, or as a result of a full sea ice cover. To investigate this further, we study the 4DEG experiment with transient changes in sea ice volume. In the 4DEG experiment the NMOC varies between 2 Sv ($1 \text{ Sv} = 10^6 \text{ m}^3 \text{ s}^{-1}$) in the state with maximum sea ice and 6 Sv in the state with minimum sea ice. As T_A is kept constant throughout the experiment, the shift in the strength of the NMOC is due to sea ice changes and not to changes in the inflowing Atlantic water. In contrast, the 5DEG experiment has a maximum NMOC of 6 Sv (Table 1), suggesting that the largest part of the decrease in NMOC from the WARM to the COLD state is due to the presence of a sea ice cover and not to changes in T_A (i.e., buoyancy forcing). However, as with the total heat transport, there is a close to linear increase in the overturning with T_A for the WARM experiments,

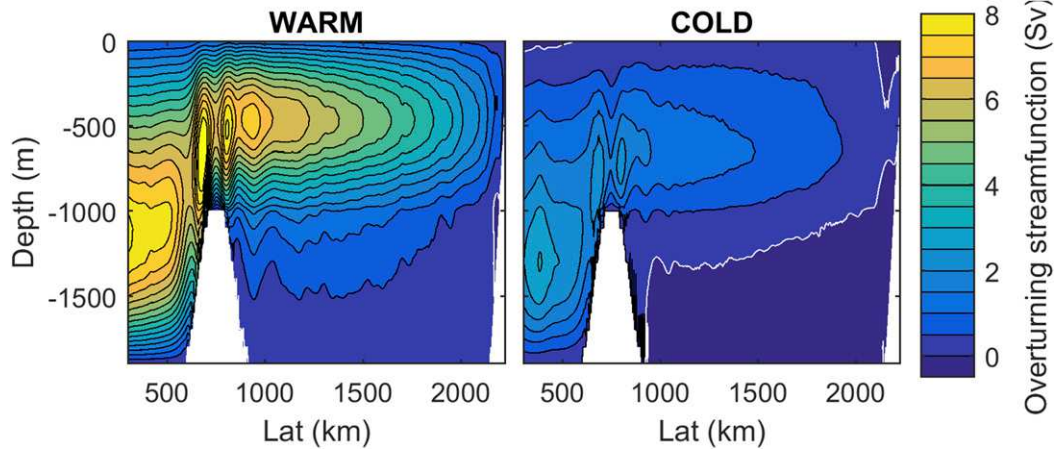


FIG. 11. Meridional overturning streamfunction for WARM (6DEG) and COLD (3DEG) in contours. White lines mark the zero contour. The overturning circulation decreases for the COLD experiments.

showing the importance of buoyancy forcing when sea ice is at a minimum. The linear relationship agrees with the theory developed by Spall (2012), where the circulation scales with the difference between inflowing temperature and the atmospheric temperature.

The effect of a full sea ice cover and reduced heat loss to the atmosphere is a decrease in downwelling and mixed layer depths (Figs. 9 and 12), contributing to the decreasing NMOC. We note that a deep negative

overturning cell is present for the COLD experiments, likely a result of increased brine rejection from enhanced sea ice formation. In addition, the temperature of the deep water that exits the Nordic seas across the sill decreases with a full sea ice cover.

d. Theoretical solutions

There is a nonlinear relationship between the Atlantic water temperature and the sea ice volume (Fig. 5). All

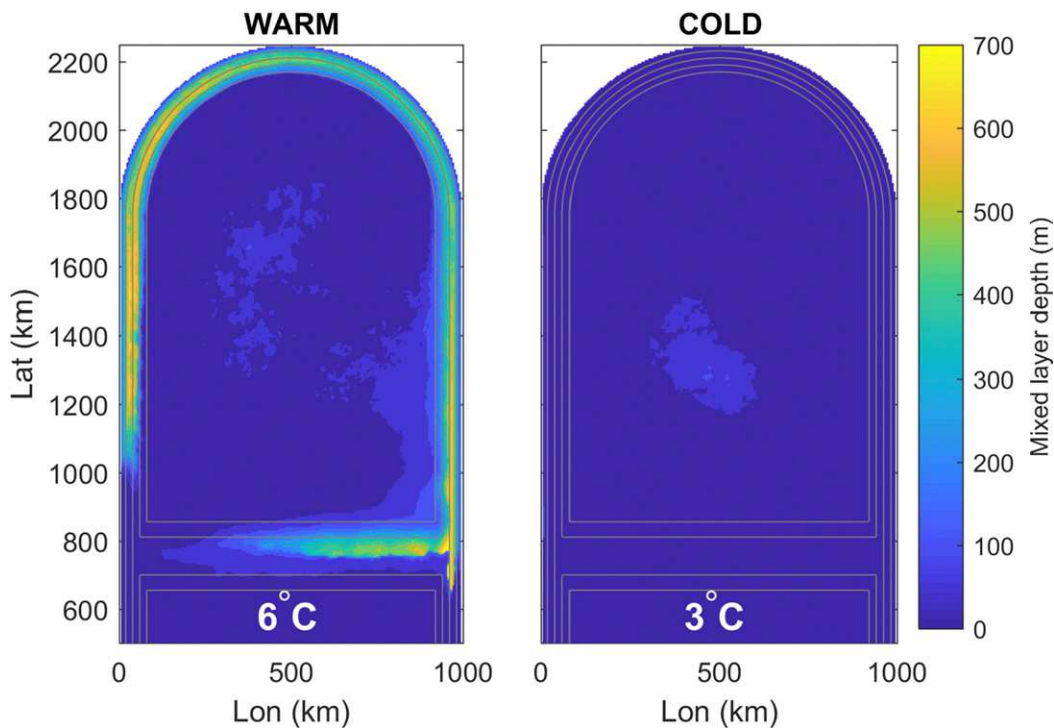


FIG. 12. Colors show mixed layer depths for 6DEG (WARM) and 3DEG (COLD). Gray lines are bathymetry. The mixed layer depth decreases for the COLD experiments.

experiments with $T_A < 4^\circ\text{C}$ resemble the COLD state, while the experiments with $T_A > 4^\circ\text{C}$ resemble the WARM state. At 4°C , the experiment shifts between the WARM and the COLD state. The limit between the two states is set by whether sea ice can expand over the boundary current or not, which again depends on the parameters chosen. For example, if the atmospheric temperature forcing increases, the limit between WARM and COLD experiments shifts to lower T_A .

1) ATMOSPHERIC COOLING

The sea ice melts if the ocean heat flux F_w into the ice is larger than the conductive heat flux F_c through the ice; F_c is balanced by the atmospheric fluxes F_{atm} . In steady state,

$$F_w = F_c = F_{\text{atm}} = F_{\text{LW}\uparrow} - F_{\text{LW}\downarrow}. \quad (2)$$

Here,

$$c_p \rho_0 (T_0 - T_f) u^* = \frac{\lambda}{h_i} (T_f - T_s) = \varepsilon \sigma T_{sk}^4 - F_{\text{LW}\downarrow}, \quad (3)$$

where T_0 is the temperature of the surface layer, T_f is the freezing temperature of seawater, u^* is a mixing efficiency constant, h_i is the sea ice thickness, λ is the thermal conductivity of the sea ice, T_s and T_{sk} are the surface temperature of the sea ice in degrees Celsius and kelvin, respectively, ε is the emissivity of sea ice, and σ is the Stefan–Boltzmann constant. Equation (3) allows for very small differences between T_0 and T_f [$O(0.1)^\circ\text{C}$].

2) SEA SURFACE TEMPERATURE

Equation (3) can be solved for T_s and h_i given T_0 . In the beginning of the simulations and in the absence of sea ice, the surface temperature of the interior is determined by eddy heat fluxes from the south and the boundary current and by atmospheric cooling. Therefore, T_0 can be solved from

$$PH\overline{vT_0} = \frac{\Gamma A(T_0 - T_{\text{atm}})}{\rho_0 c_p}, \quad (4)$$

where P is the perimeter of the boundary current or the sill crest, A is the area of the region, T_{atm} is the atmospheric temperature, and Γ is a relaxation constant. Following Visbeck et al. (1996) and Spall (2004, 2012, 2013), we parameterize the eddy heat fluxes as being proportional to the baroclinic velocity in the boundary current V , and the temperature–salinity difference between the interior and boundary current/southern region. Assuming small salinity differences, the eddy heat fluxes can be parameterized as

$$\overline{vT_0} = cV(T_A - T_0) = \frac{cgH(T_A - T_0)}{\rho_0 f_0 L} [\alpha(T_A - T_0)], \quad (5)$$

and T_0 solved from

$$\frac{PcgH^2}{\rho_0 f_0 L} [\alpha(T_A - T_0)^2] = \frac{\Gamma A(T_0 - T_{\text{atm}})}{\rho_0 c_p}, \quad (6)$$

where c is a nondimensional coefficient, g is the gravitational acceleration, L is the width over the sloping topography, and α is the thermal expansion coefficient. Solving Eq. (6) for the area just north of the sill, the balance predicts the surface temperatures for the WARM experiments (Fig. 13). However, the balance does not apply to the cold sea ice–covered state where surface temperatures are close to freezing.

3) SEA ICE MELT

We also calculate how much sea ice must melt to produce a fresh surface layer with freezing temperatures that is lighter than the Atlantic water for each experiment. First we calculate the highest possible sea surface salinity S_0 , which gives $\rho_0 < \rho_A$, where $\rho_A = \rho(S_A = 35, T_A = T_A)$ and $T_0 = -1.9^\circ\text{C}$. Then, given a sea ice salinity of S_i , we calculate the fraction of this water, f_0 , needed to mix with Atlantic water S_A to produce water with $S = S_0$:

$$f_0 + f_A = 1, \quad (7)$$

$$\rho_0 S_0 = f_0 \rho_{\text{ice}} S_i + f_A \rho_0 S_A, \quad (8)$$

which gives

$$f_0 = \rho_0 \frac{S_0 - S_A}{\rho_{\text{ice}} S_i - \rho_0 S_A}, \quad (9)$$

where ρ_{ice} is the density of sea ice. As the horizontal areas of the grid cells are the same, the sea ice thickness needed to melt to make the surface layer with a constant depth h_1 sufficiently light is

$$h_i = h_1 \rho_0 \frac{S_0 - S_A}{\rho_{\text{ice}} S_i - \rho_0 S_A}. \quad (10)$$

More ice needs to melt to create a light enough surface layer for the WARM experiments compared to the COLD experiments (Fig. 13b). Noticeably, the sea ice thickness that needs to melt for a stable stratification is larger than the mean sea ice thickness of the WARM experiments and so no halocline can be supported in this parameter range.

4. Discussion

By applying an idealized setup of the MITgcm we show that a full sea ice cover can exist in a Nordic seas–like domain together with an active Atlantic inflow. However, for a full sea ice cover to be present, the

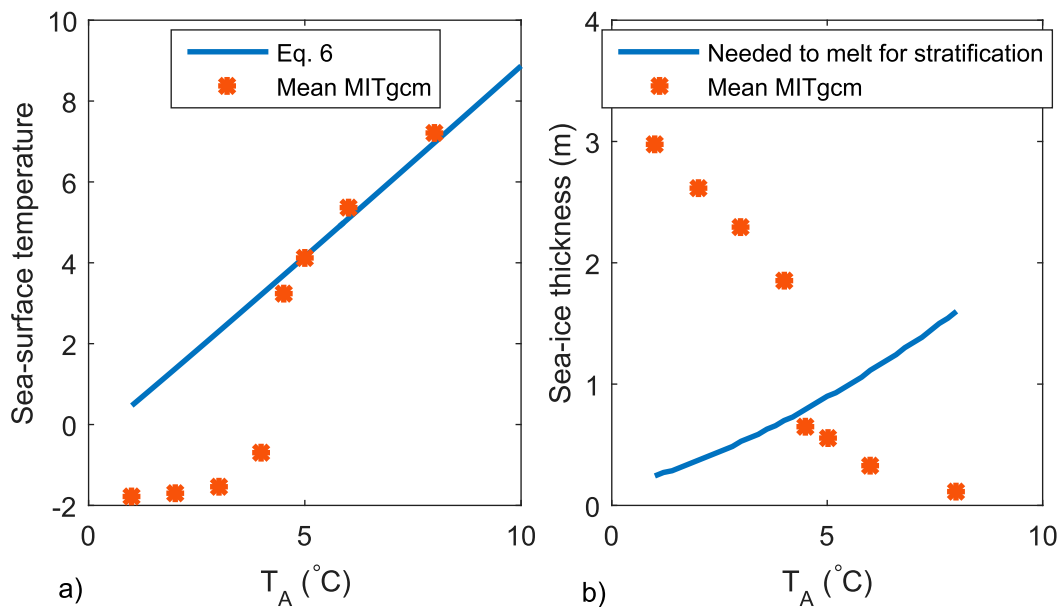


FIG. 13. (a) Sea surface temperatures ($^{\circ}\text{C}$) calculated from Eq. (6) and from the MITgcm (mean, 50–125 km north of GSR). (b) Ice thickness needed to melt to create a stable fresh surface layer and mean sea ice thickness from the MITgcm experiments north of the sill.

temperature of the Atlantic water needs to be reduced, as well as the heat transport to the Nordic seas. As a consequence, there is a subtle balance between the warm north-flowing Atlantic water, a fresh surface layer, and extensive sea ice formation in the Nordic seas.

The existence of a self-sustained sea ice cover in the Nordic seas is relevant for the large-scale climate variability of the last glacial period where a temporal Nordic seas sea ice cover is hypothesized to govern the abrupt temperature fluctuations recorded in Greenland ice cores. An external freshwater supply is often assumed to be present for a sea ice cover to exist in the Nordic seas. This has typically been attributed to freshwater input from the Laurentide Ice Sheet during stadials (e.g., Broecker et al. 1990; Manabe and Stouffer 1995), enhanced runoff from the Fennoscandian Ice Sheet during interstadials (Dokken et al. 2013), or enhanced ice export from the Arctic Ocean (Tarasov and Peltier 2005). For the first case, runoff is assumed to be largest during cold stadial periods. This is problematic as freshwater is needed the most when the climate state is the least supportive of melting. In addition, episodic freshwater input from the Laurentide Ice Sheet is mainly associated with Heinrich stadials, and not every stadial period.

Here we show that a sea ice cover and Arctic-like stratification can exist without an external freshwater supply. Under sufficiently cold conditions, a halocline, capped by sea ice, emerges spontaneously. The presence

of an intermittent freshwater source during the last glacial period is therefore not necessary to explain the cold fresh surface layer that proxy data suggest was present during Greenland stadials. We do note that the Arctic-like stratification also emerges in the presence of external freshwater inputs. Sensitivity studies with a virtual freshwater flux along the eastern margin of the model domain demonstrate that additional freshwater aids in the formation of a halocline. However, the non-linear transition between the WARM and COLD states still exists; it just moves to slightly higher Atlantic water temperatures.

The unforced halocline formation also has implications for the modern Arctic Ocean. It is debated whether the cold halocline is formed by the addition and advection of cold and salty water produced by sea ice formation on shallow shelves (Aagaard et al. 1981), or by convection in the deep ocean during winter and the addition of freshwater from river runoff and sea ice melt to the surface (Rudels et al. 1996). A halocline is assumed to be a prerequisite for a sea ice cover to exist. Here we show that processes similar to those proposed by Rudels et al. (1996) can, under the present idealized configuration, create a halocline. However, freshwater from river runoff is not needed. Similar to modern oceanographic observations north of Svalbard (Rudels et al. 2005), the Atlantic water cools by heat loss and sea ice melt. The sea ice melt is mainly a seasonal signal (Rudels et al. 2005; Pemberton et al. 2015), but we show that sea ice melt also occurs under cold conditions

associated with winter. As cold conditions are crucial for the stability of the halocline, the observed warming of the Atlantic water in recent decades (Polyakov et al. 2005, 2012) might have profound implications for the stability of Arctic sea ice cover.

The highly nonlinear response in sea ice volume to Atlantic water temperatures suggests that large changes in sea ice could occur with small changes within a given range of Atlantic water temperatures. Several studies have shown that the variability of the climate system depends on the background climate state (e.g., Ganopolski and Rahmstorf 2001; Bitz et al. 2007), with less variability in a cold climate than in an intermediate climate. This has typically been related to the recovery rate of the thermohaline circulation after a shutdown resulting from freshwater input (Rahmstorf 1996; Stouffer et al. 2006; Bitz et al. 2007). However, sea ice expansion, a stronger stratification, and additional surface freshwater input through seasonal melt have been shown to affect the recovery rate and hence contribute to a more stable climate in a cold state (Bitz et al. 2007). Also, ice-core records (Dansgaard et al. 1982, 1993) show more variability during intermediate climates; the DO events are present in Marine Isotope Stage 3 (MIS3), which is warmer than the more stable Last Glacial Maximum and colder than the much more stable Holocene. In addition, cold stadials are typically more stable than interstadial periods. In our coldest experiments (1DEG–3DEG), the sea ice cover in the Nordic seas is very stable and the temperature of the Atlantic water must increase by a couple of degrees to trigger a transition into a warm state with significant changes in ice cover. However, this is not the case for the intermediate experiments (e.g., 4DEG), where a small warming of the incoming Atlantic water provides a rapid transition into the warm state with dramatic changes in sea ice cover and heat transport.

This suggests that given the appropriate background climate, such as MIS3 during the last glacial period, a small change in ocean circulation and heat transport into the Nordic seas could have large consequences for the Nordic seas and surrounding climate. This oceanic change could involve larger-scale changes to, for example, the AMOC or more local changes to, for example, the horizontal circulation and the subpolar gyre, which are seen to have large effects on the heat transport into the Nordic seas (Boccaletti et al. 2005; Hátún et al. 2005). For the 4DEG experiment, transient changes in sea ice are even present without a change in the incoming Atlantic water, suggesting that large sea ice variability could also be intrinsic to an intermediate climate state. The observed link between sea ice variability and the background climate state in both models and observations could explain why larger variability is found in the North

Atlantic during the intermediate climate state of MIS3 than during colder and warmer periods of the past.

a. *Limitations of the model*

The seasonal cycle is a key mechanism missing in this study. The seasonal variability of sea ice could prevent abrupt reductions in sea ice cover (Tietsche et al. 2011). In particular, seasonal sea ice would enhance the stratification because of melting and freshwater release during summer, and sea ice production and brine rejection during winter. Therefore, we expect the transition between the COLD and the WARM state of the model to occur at higher Atlantic water temperatures if seasonality were to be included as more sea ice melt would occur. On the other hand, the consequent change in heat content of the ocean could prevent sea ice formation and shift the limit to lower temperatures. A follow up to this study will therefore include a representation of the seasonal cycle in the climate forcing.

In our experiments, the meridional overturning circulation decreases as a consequence of increasing sea ice cover in the Nordic seas. However, we note that this is the local overturning in the Nordic seas (i.e., NMOC) only, and not the full AMOC. There is a constant supply of warm salty water in the south of the domain, which is not sensitive to changes in the NMOC. We are thus not representing the NMOC's potential impact on the circulation farther south. In reality, the circulation changes in the Nordic seas have the potential to impact the global circulation. However, it is not clear whether changes in the NMOC would affect the AMOC, and this relationship needs to be further investigated. If AMOC weakened, it could lead to a reinforcement of the sea ice cover as a reduced AMOC is associated with a smaller heat transport into the Nordic seas. However, the heat transport by the subpolar gyre could compensate, or also be affected by the sea ice cover resulting from, for example, wind or density changes (Born and Levermann 2010; Born et al. 2015).

For simplicity we have ignored the effects of wind in this study and, as shown by Spall (2011), adding wind forcing representative of the present climate has little effect on the net heat transport to the Nordic seas. However, significant changes in the wind fields are thought to have occurred during parts of the last glacial period when the ice sheets and sea ice were different from today (Löfverström et al. 2014). Evidence showing large changes in the dust content in the ice cores on Greenland between stadial and interstadial transitions suggests significant changes to the atmospheric circulation during MIS3 (Mayewski et al. 1994). In addition to the potential for changes in the wind forcing through time, the impact of wind in general on the sea ice cover could be important and should be considered in further studies.

As discussed, the dynamic component of the sea ice model is required in order to advect sea ice out of the interior of the basin, and produce a full sea ice cover in the Nordic seas. The presence of a northerly or westerly wind is likely to further promote the formation of a full sea ice cover as it would move the sea ice into the warm boundary current, thereby enhancing sea ice melt, surface freshening, and farther sea ice expansion. Winds would also enhance the turbulent mixing of the ocean, especially over the open ocean. However, we performed sensitivity experiments with increased vertical diffusion, which show little effect on the results, suggesting that the potential increase in vertical mixing with winds would have limited effect on these experiments.

Further studies will focus on the unforced oscillations of the 4DEG experiment. We expect the time scale of the oscillations to change depending on the complexity of the model. In the current model version, the decadal time scale of the unforced oscillations does not compare to the millennial-scale variability observed in glacial climate records. However, the time scales of the unforced oscillations are expected to change when a seasonal cycle is included, as well as feedback with the larger-scale global ocean circulation.

b. Concluding remarks

As noted by Spall (2011), eddy heat fluxes are crucial for a correct representation of the net heat exchange across the sill crest, and thus need to be resolved or parameterized in climate models for a correct representation of the heat transport. We note that the same is true for the advection of sea ice, which is dominated by eddy fluxes at low sea ice cover. Representation of these processes is key to the results presented in this study, which suggests caution should be considered in analyzing similar mechanisms in climate models that are not eddy resolving. In particular, the sensitivity of IPCC-type models to potential future changes in the temperature of inflowing Atlantic water to the Arctic should be analyzed with this in mind.

In this study, a full sea ice cover leads to a reduction in the outgoing heat from the ocean to the atmosphere, a reduction in the overturning streamfunction, and a reduction in the heat transport to the Nordic seas. However, all of the above also decrease with a reduction in buoyancy forcing resulting from decreasing Atlantic water temperatures. As a full sea ice cover develops with a decrease in Atlantic water temperature, the observed changes in circulation could be a result of the decreasing buoyancy forcing. However, the changes are larger with the sea ice transition and show a nonlinear behavior. In addition, Spall (2012) shows periods of reduced convection, overturning circulation, and northward heat transport in similar experiments where the Atlantic water temperature is kept

constant. The circulation changes are due to external freshwater input and the establishment of a freshwater cap in the interior that shuts down convection. These points support our conclusion that expansion of sea ice in the Nordic seas is a key player in the circulation changes.

Reconstructions from marine sediments suggest that there were significant changes in the circulation of the Nordic seas and North Atlantic during the stadial to interstadial transitions of the last glacial (Rasmussen et al. 1996; Kissel et al. 1999; Dokken and Jansen 1999; Henry et al. 2016; Burckel et al. 2016). Based solely on the proxy data, it is not clear whether changes in sea ice is a consequence or a cause of these reconstructed changes. However, our study using theory and dynamical models shows that abrupt transitions in Nordic seas sea ice can occur spontaneously with only small, or no, changes in forcing given the appropriate background climate.

5. Summary of key conclusions

The key conclusions are as follows:

- There is a strong nonlinear response in Nordic seas sea ice cover to Atlantic water temperatures, with the potential for large changes in sea ice given only small, or no, changes in temperature.
- A halocline and Arctic-like stratification emerge through sea ice production given low Atlantic water temperatures.
- The advection of sea ice by the mean flow and eddy fluxes is crucial for the development of the halocline.
- The presence of a freshwater source is not necessary to explain a fresh surface layer during glacial climates.
- Total heat transport to the Nordic seas and the local overturning circulation in the basin decrease with a full sea ice cover.
- Eddy heat fluxes dominate the heat exchange across the Greenland–Scotland Ridge.
- Given a full sea ice cover, warm inflowing Atlantic water retains most of its heat and recirculates as a warm western boundary current out of the Nordic seas.
- The western Nordic seas warms above 800 m and cools below given a full sea ice cover.

Acknowledgments. The research was supported by the Centre for Climate Dynamics at the Bjerknes Centre for Climate Research. The research leading to these results is part of the ice2ice project funded by the European Research Council under the European Community Seventh Framework Programme (FP7/2007-2013)/ERC Grant Agreement 610055. The simulations were performed on resources provided by UNINETT Sigma2—the National Infrastructure for High Performance Computing and Data Storage in

Norway. MAS was supported by the National Science Foundation Grants OCE-1533170 and OCE-1558742. We wish to thank Johan Nilsson and Andreas Born for insightful comments, and the anonymous reviewers for their constructive comments which improved the manuscript.

REFERENCES

- Aagaard, K., L. K. Coachman, and E. Carmack, 1981: On the halocline of the Arctic Ocean. *Deep-Sea Res.*, **28A**, 529–545, [https://doi.org/10.1016/0198-0149\(81\)90115-1](https://doi.org/10.1016/0198-0149(81)90115-1).
- Bitz, C. M., J. C. H. Chiang, W. Cheng, and J. J. Barsugli, 2007: Rates of thermohaline recovery from freshwater pulses in modern, Last Glacial Maximum, and greenhouse warming climates. *Geophys. Res. Lett.*, **34**L07708, <https://doi.org/10.1029/2006GL029237>.
- Boccaletti, G., R. Ferrari, A. Adcroft, D. Ferreira, and J. Marshall, 2005: The vertical structure of ocean heat transport. *Geophys. Res. Lett.*, **32**L10603, <https://doi.org/10.1029/2005GL022474>.
- Born, A., and A. Levermann, 2010: The 8.2 ka event: Abrupt transition of the subpolar gyre toward a modern North Atlantic circulation. *Geochem. Geophys. Geosyst.*, **11** Q06011, <https://doi.org/10.1029/2009GC003024>.
- , J. Mignot, and T. F. Stocker, 2015: Multiple equilibria as a possible mechanism for decadal variability in the North Atlantic Ocean. *J. Climate*, **28**, 8907–8922, <https://doi.org/10.1175/JCLI-D-14-00813.1>.
- Broecker, W. S., 2000: Abrupt climate change: Causal constraints provided by the paleoclimate record. *Earth-Sci. Rev.*, **51**, 137–154, [https://doi.org/10.1016/S0012-8252\(00\)00019-2](https://doi.org/10.1016/S0012-8252(00)00019-2).
- , G. Bond, M. Klas, G. Bonai, and W. Wolfli, 1990: A salt oscillator in the glacial Atlantic? 1. The concept. *Paleoceanography*, **5**, 469–477, <https://doi.org/10.1029/PA005i004p00469>.
- Burckel, P., and Coauthors, 2016: Changes in the geometry and strength of the Atlantic meridional overturning circulation during the last glacial (20–50 ka). *Climate Past*, **12** 2061–2075, <https://doi.org/10.5194/cp-12-2061-2016>.
- Dansgaard, W., H. B. Clausen, N. Gundestrup, C. U. Hammer, S. F. Johnsen, P. M. Kristinsdottir, and N. Reeh, 1982: A new Greenland deep ice core. *Science*, **218**, 1273–1277, <https://doi.org/10.1126/science.218.4579.1273>.
- , and Coauthors, 1993: Evidence for general instability of past climate from a 250-kyr ice-core record. *Nature*, **364**, 218–220, <https://doi.org/10.1038/364218a0>.
- Dokken, T. M., and E. Jansen, 1999: Rapid changes in the mechanism of ocean convection during the last glacial period. *Nature*, **401**, 458–461, <https://doi.org/10.1038/46753>.
- , K. H. Nisancioglu, C. Li, D. S. Battisti, and C. Kissel, 2013: Dansgaard-Oeschger cycles: Interactions between ocean and sea intrinsic to the Nordic seas. *Paleoceanography*, **28**, 491–502, <https://doi.org/10.1002/palo.20042>.
- Eynaud, F., and Coauthors, 2009: Position of the polar front along the western Iberian margin during key cold episodes of the last 45 ka. *Geochem. Geophys. Geosyst.*, **10**, Q07U05, <https://doi.org/10.1029/2009GC002398>.
- Ezat, M. M., T. L. Rasmussen, and J. Groeneveld, 2014: Persistent intermediate water warming during cold stadials in the southeastern Nordic seas during the past 65 k.y. *Geology*, **42**, 663–666, <https://doi.org/10.1130/G35579.1>.
- Gade, H. G., 1979: Melting of ice in sea water: A primitive model with application to the Antarctic ice shelf and icebergs. *J. Phys. Oceanogr.*, **9**, 189–198, [https://doi.org/10.1175/1520-0485\(1979\)009<0189:MOIISW>2.0.CO;2](https://doi.org/10.1175/1520-0485(1979)009<0189:MOIISW>2.0.CO;2).
- Ganopolski, A., and S. Rahmstorf, 2001: Rapid changes of glacial climate simulated in a coupled climate model. *Nature*, **409**, 153–158, <https://doi.org/10.1038/35051500>.
- Gildor, H., and E. Tziperman, 2003: Sea-ice switches and abrupt climate change. *Philos. Trans. Roy. Soc. London*, **361**, 1935–1944, <https://doi.org/10.1098/rsta.2003.1244>.
- Grootes, P. M., and M. Stuiver, 1997: Oxygen 18/16 variability in Greenland snow and ice with 10³- to 10⁵-year time resolution. *J. Geophys. Res.*, **102**, 26 455–26 470, <https://doi.org/10.1029/97JC00880>.
- Hansen, B., and S. Østerhus, 2000: North Atlantic–Nordic seas exchanges. *Prog. Oceanogr.*, **45**, 109–208, [https://doi.org/10.1016/S0079-6611\(99\)00052-X](https://doi.org/10.1016/S0079-6611(99)00052-X).
- Hátún, H., A. B. Sandø, H. Drange, B. Hansen, and H. Valdimarsson, 2005: Influence of the Atlantic Subpolar Gyre on the thermohaline circulation. *Science*, **309**, 1841–1844, <https://doi.org/10.1126/science.1114777>.
- Henry, L. G., J. F. McManus, W. B. Curry, N. L. Roberts, A. M. Piotrowski, and L. D. Keigwin, 2016: North Atlantic Ocean circulation and abrupt climate change during the last glaciation. *Nature*, **353**, 470–474, <https://doi.org/10.1126/science.aaf5529>.
- Hibler, W. D., III, 1980: Modeling a variable thickness sea ice cover. *Mon. Wea. Rev.*, **108**, 1943–1973, [https://doi.org/10.1175/1520-0493\(1980\)108<1943:MAVTSI>2.0.CO;2](https://doi.org/10.1175/1520-0493(1980)108<1943:MAVTSI>2.0.CO;2).
- Hoff, U., T. L. Rasmussen, R. Stein, M. M. Ezat, and K. Fahl, 2016: Sea ice and millennial-scale climate variability in the Nordic seas 90 kyr ago to present. *Nat. Commun.*, **7**, 12247, <https://doi.org/10.1038/ncomms12247>.
- Jackett, D. R., and T. J. McDougall, 1995: Minimal adjustment of hydrographic profiles to achieve static stability. *J. Atmos. Oceanic Technol.*, **12**, 381–389, [https://doi.org/10.1175/1520-0426\(1995\)012<0381:MAOHP>2.0.CO;2](https://doi.org/10.1175/1520-0426(1995)012<0381:MAOHP>2.0.CO;2).
- Jensen, M. F., 2017: Abrupt changes in sea ice and dynamics of Dansgaard-Oeschger events. Ph.D. thesis, University of Bergen, 139 pp.
- , J. Nilsson, and K. H. Nisancioglu, 2016: The interaction between sea ice and salinity-dominated ocean circulation: Implications for halocline stability and rapid changes of sea ice cover. *Climate Dyn.*, **47**, 3301–3317, <https://doi.org/10.1007/s00382-016-3027-5>.
- Johnsen, S. J., and Coauthors, 1992: Irregular glacial interstadials recorded in a new Greenland ice core. *Nature*, **359**, 311–313, <https://doi.org/10.1038/359311a0>.
- Kissel, C., C. Laj, L. Labeyrie, T. Dokken, A. Voelker, and D. Blamart, 1999: Rapid climatic variations during marine isotope stage 3: Magnetic analysis of sediments from Nordic seas and North Atlantic. *Earth Planet. Sci. Lett.*, **171**, 489–502, [https://doi.org/10.1016/S0012-821X\(99\)00162-4](https://doi.org/10.1016/S0012-821X(99)00162-4).
- Li, C., D. S. Battisti, D. P. Schrag, and E. Tziperman, 2005: Abrupt climate shifts in Greenland due to displacements of the sea ice edge. *Geophys. Res. Lett.*, **32**, L19702, <https://doi.org/10.1029/2005GL023492>.
- , —, and C. M. Bitz, 2010: Can North Atlantic sea ice anomalies account for Dansgaard-Oeschger climate signals? *J. Climate*, **23**, 5457–5475, <https://doi.org/10.1175/2010JCLI3409.1>.
- Löfverström, M., R. Caballero, J. Nilsson, and J. Kleman, 2014: Evolution of the large-scale atmospheric circulation in response to changing ice sheets over the last glacial cycle. *Climate Past*, **10**, 1453–1471, <https://doi.org/10.5194/cp-10-1453-2014>.
- Losch, M., D. Menemenlis, J.-M. Campin, P. Heimbach, and C. Hill, 2010: On the formulation of sea-ice models. Part 1: Effects of different solver implementations and parameterizations.

- Ocean Modell.*, **33**, 129–144, <https://doi.org/10.1016/j.ocemod.2009.12.008>.
- Manabe, S., and R. J. Stouffer, 1995: Simulation of abrupt climate change induced by freshwater input to the North Atlantic Ocean. *Nature*, **378**, 165–167, <https://doi.org/10.1038/378165a0>.
- Marotzke, J., 2000: Abrupt climate change and the thermohaline circulation: Mechanisms and predictability. *Proc. Natl. Acad. Sci. USA*, **97**, 1347–1350, <https://doi.org/10.1073/pnas.97.4.1347>.
- Masson-Delmotte, V., and Coauthors, 2005: GRIP deuterium excess reveals rapid and orbital-scale changes in Greenland moisture origin. *Science*, **309**, 118–121, <https://doi.org/10.1126/science.1108575>.
- Mayewski, P. A., and Coauthors, 1994: Changes in atmospheric circulation and ocean ice cover over the North Atlantic during the last 41,000 years. *Science*, **263**, 1747–1751, <https://doi.org/10.1126/science.263.5154.1747>.
- North Greenland Ice Core Project members, 2004: High-resolution record of Northern Hemisphere climate extending into the last interglacial period. *Nature*, **431**, 147–151, <https://doi.org/10.1038/nature02805>.
- Orvik, K. A., and P. Niiler, 2002: Major pathways of Atlantic water in the northern North Atlantic and Nordic seas toward Arctic. *Geophys. Res. Lett.*, **29**, 1896, <https://doi.org/10.1029/2002GL015002>.
- , Ø. Skagseth, and M. Mork, 2001: Atlantic inflow to the Nordic seas: Current structure and volume fluxes from moored current meters, VM-ADCP and SeaSoar-CTD observations, 1995–1999. *Deep-Sea Res.*, **48**, 937–957, [https://doi.org/10.1016/S0967-0637\(00\)00038-8](https://doi.org/10.1016/S0967-0637(00)00038-8).
- Pemberton, P., J. Nilsson, M. Hieronymus, and H. E. M. Meier, 2015: Arctic Ocean water mass transformation in *S–T* coordinates. *J. Phys. Oceanogr.*, **45**, 1025–1050, <https://doi.org/10.1175/JPO-D-14-0197.1>.
- Polyakov, I. V., and Coauthors, 2005: One more step toward a warmer Arctic. *Geophys. Res. Lett.*, **32**, L17605, <https://doi.org/10.1029/2005GL023740>.
- , A. V. Pnyushkov, and L. A. Timokhov, 2012: Warming of the Intermediate Atlantic Water of the Arctic Ocean in the 2000s. *J. Climate*, **25**, 8362–8370, <https://doi.org/10.1175/JCLI-D-12-00266.1>.
- Rahmstorf, S., 1996: On the freshwater forcing and transport of the Atlantic thermohaline circulation. *Climate Dyn.*, **12**, 799–811, <https://doi.org/10.1007/s003820050144>.
- , 2002: Ocean circulation and climate during the past 120,000 years. *Nature*, **419**, 207–214, <https://doi.org/10.1038/nature01090>.
- Rasmussen, T. L., and E. Thomsen, 2004: The role of the North Atlantic drift in the millennial timescale glacial climate fluctuations. *Palaeogeogr. Palaeoclimatol. Palaeoecol.*, **210**, 101–116, <https://doi.org/10.1016/j.palaeo.2004.04.005>.
- , —, L. Labeyrie, and T. C. E. van Weering, 1996: Circulation changes in the Faeroe-Shetland Channel correlating with cold events during the last glacial period (58–10 ka). *Geology*, **24**, 937–940, [https://doi.org/10.1130/0091-7613\(1996\)024<0937:CCITFS>2.3.CO;2](https://doi.org/10.1130/0091-7613(1996)024<0937:CCITFS>2.3.CO;2).
- , —, and M. Moros, 2016: North Atlantic warming during Dansgaard-Oeschger events synchronous with Antarctic warming and out-of-phase with Greenland climate. *Sci. Rep.*, **6**, 20535, <https://doi.org/10.1038/srep20535>.
- Rudels, B., L. G. Anderson, and E. P. Jones, 1996: Formation and evolution of the surface mixed layer and halocline of the Arctic Ocean. *J. Geophys. Res.*, **101**, 8807–8821, <https://doi.org/10.1029/96JC00143>.
- , G. Björk, J. Nilsson, P. Winsor, I. Lake, and C. Nohr, 2005: The interaction between waters from the Arctic Ocean and the Nordic seas north of Fram Strait and along the East Greenland Current: Results from the Arctic Ocean-02 Oden expedition. *J. Mar. Syst.*, **55**, 1–30, <https://doi.org/10.1016/j.jmarsys.2004.06.008>.
- Sánchez Goñi, M. F., A. Landais, W. J. Fletcher, F. Naughton, S. Desprat, and J. Duprat, 2008: Contrasting impacts of Dansgaard-Oeschger events over a western European latitudinal transect modulated by orbital parameters. *Quat. Sci. Rev.*, **27**, 1136–1151, <https://doi.org/10.1016/j.quascirev.2008.03.003>.
- Seidov, D., O. K. Baranova, M. Biddle, T. P. Boyer, D. R. Johnson, A. V. Mishonov, C. Paver, and M. Zweng, 2013: Greenland-Iceland-Norwegian Seas Regional Climatology (NODC Accession 0112824), version 3.5. NOAA National Oceanographic Data Center, accessed 23 May 2017, <https://doi.org/10.7289/V5GT5K30>.
- , and Coauthors, 2015: Oceanography north of 60°N from World Ocean Database. *Prog. Oceanogr.*, **132**, 153–173, <https://doi.org/10.1016/j.pocean.2014.02.003>.
- Smagorinsky, J., 1963: General circulation experiments with the primitive equations. *Mon. Wea. Rev.*, **91**, 99–164, [https://doi.org/10.1175/1520-0493\(1963\)091<0099:GCEWTP>2.3.CO;2](https://doi.org/10.1175/1520-0493(1963)091<0099:GCEWTP>2.3.CO;2).
- Spall, M. A., 2004: Boundary current and watermass transformation in marginal seas. *J. Phys. Oceanogr.*, **34**, 1197–1213, [https://doi.org/10.1175/1520-0485\(2004\)034<1197:BCAWTI>2.0.CO;2](https://doi.org/10.1175/1520-0485(2004)034<1197:BCAWTI>2.0.CO;2).
- , 2011: On the role of eddies and surface forcing in the heat transport and overturning circulation in marginal seas. *J. Climate*, **24**, 4844–4858, <https://doi.org/10.1175/2011JCLI4130.1>.
- , 2012: Influences of precipitation on water mass transformation and deep convection. *J. Phys. Oceanogr.*, **42**, 1684–1700, <https://doi.org/10.1175/JPO-D-11-0230.1>.
- , 2013: On the circulation of Atlantic water in the Arctic Ocean. *J. Phys. Oceanogr.*, **43**, 2352–2371, <https://doi.org/10.1175/JPO-D-13-079.1>.
- Stouffer, R. J., and Coauthors, 2006: Investigating the causes of the response of the thermohaline circulation to past and future climate changes. *J. Climate*, **19**, 1365–1387, <https://doi.org/10.1175/JCLI3689.1>.
- Tarasov, L., and W. R. Peltier, 2005: Arctic freshwater forcing of the Younger Dryas cold reversal. *Nature*, **435**, 662–665, <https://doi.org/10.1038/nature03617>.
- Tietsche, S., D. Notz, J. H. Jungclauss, and J. Marotzke, 2011: Recovery mechanisms of Arctic summer sea ice. *Geophys. Res. Lett.*, **38**, L02707, <https://doi.org/10.1029/2010GL045698>.
- Tziperman, E., 1997: Inherently unstable climate behaviour due to weak thermohaline ocean circulation. *Nature*, **386**, 592–595, <https://doi.org/10.1038/386592a0>.
- Visbeck, M., J. Marshall, and H. Jones, 1996: Dynamics of isolated convective regions in the ocean. *J. Phys. Oceanogr.*, **26**, 1721–1734, [https://doi.org/10.1175/1520-0485\(1996\)026<1721:DOICRI>2.0.CO;2](https://doi.org/10.1175/1520-0485(1996)026<1721:DOICRI>2.0.CO;2).
- Voelker, A. H. L., 2002: Global distribution of centennial-scale records for Marine Isotope Stage (MIS) 3: A database. *Quat. Sci. Rev.*, **21**, 1185–1212, [https://doi.org/10.1016/S0277-3791\(01\)00139-1](https://doi.org/10.1016/S0277-3791(01)00139-1).
- , and L. de Abreu, 2013: A review of abrupt climate change events in the northeastern Atlantic Ocean (Iberian Margin): Latitudinal, longitudinal, and vertical gradients. *Abrupt Climate Change: Mechanisms, Patterns, and Impacts*, *Geophys. Monogr.*, Vol. 193, Amer. Geophys. Union, 15–37.
- Walín, G., G. Broström, J. Nilsson, and O. Dahl, 2004: Baroclinic boundary currents with downstream decreasing buoyancy: A study of an idealized Nordic seas system. *J. Mar. Res.*, **62**, 517–543, <https://doi.org/10.1357/0022240041850048>.
- Zhang, J., and W. D. Hibler III, 1997: On an efficient numerical method for modeling sea ice dynamics. *J. Geophys. Res.*, **102**, 8691–8702, <https://doi.org/10.1029/96JC03744>.